Plasmaspheric plumes: CRRES observations of enhanced density beyond the plasmapause

M. B. Moldwin,[1] J. Howard,[2] J. Sanny,[2] J. D. Bocchicchio,[3] H. K. Rassoul,[3] and R. R. Anderson[4,5]

Received 13 November 2003; revised 4 March 2004; accepted 15 March 2004; published 4 May 2004.

[1] CRRES plasma wave receiver density data were used to study the distribution and properties of dense plasmaspheric-like plasma observed outside the plasmapause. Our study indicates that outer plasmaspheric structure, often called plasmaspheric plumes, blobs, tails, or detached plasma regions, can exist at all local times under all levels of geomagnetic activity. Of the 558 CRRES orbits that had at least one clearly defined plasmapause, 169 (or 30%) had plasmaspheric-like density structures at higher L shells than the plasmapause. Most of the occurrences of plasmaspheric-like plasma observed by CRRES were in the noon-to-dusk sector in the aftermath of enhanced geomagnetic activity consistent with plasmaspheric plume models. *INDEX TERMS:* 2768 Magnetospheric Physics: Plasmasphere; 2730 Magnetospheric Physics: Magnetosphere—inner; 2760 Magnetospheric Physics: Plasma convection; 2788 Magnetospheric Physics: Storms and substorms; *KEYWORDS:* plasmasphere, plasmaspheric plumes, plasmapause, inner magnetospheric density structure

Citation: Moldwin, M. B., J. Howard, J. Sanny, J. D. Bocchicchio, H. K. Rassoul, and R. R. Anderson (2004), Plasmaspheric plumes: CRRES observations of enhanced density beyond the plasmapause, *J. Geophys. Res.*, *109*, A05202, doi:10.1029/2003JA010320.

1. Introduction

[2] Early in the development of plasmapause modeling it was recognized that long plasmaspheric plumes would develop because of enhanced convection sweeping the outer layers of the plasmasphere sunward (e.g., *Chen and Wolf* [1972]; *Chen and Grebowsky* [1978]; see also brief review paper by *Lemaire* [2000]). A number of satellite missions that had the ability to measure the thermal density of the inner magnetosphere commonly observed dense plasmaspheric-like plasma beyond the plasmapause [e.g., *Taylor et al.*, 1970; *Chappell*, 1974; *Higel and Lei*, 1984; *Carpenter et al.*, 1993; *Moldwin et al.*, 1994]. These observations, in general, fit the simple bulge or plume model of the plasmasphere [e.g., *Chen and Wolf*, 1972; *Higel and Lei*, 1984] in which the duskside bulge or plume region rotated from dusk toward noon during increasing geomagnetic activity [e.g., *Elphic et al.*, 1996] and rotated toward midnight during quiet times. Figure 1 shows the *Grebowsky* [1970] model results that have been used to explain dense plasmaspheric plasma beyond the plasmapause. The main question that could not be resolved from in situ observations is whether the dense plasmaspheric plasma is detached from the plasmasphere (blobs) or is an extension (plumes) from the main plasmasphere. The answer has ramifications for the generation of the kilometric continuum [e.g., *Green et al.*, 2002] and general plasmapause modeling studies [e.g., *O'Brien and Moldwin*, 2003]. The International Monitor for Auroral Geomagnetic Effects (IMAGE) EUV observations of global plasmaspheric morphology routinely show the creation or presence of plasmaspheric plumes [e.g., *Sandel et al.*, 2001; *Goldstein et al.*, 2003; *Garcia et al.*, 2003]. These observations are therefore supportive of the connected plume picture as opposed to the detached blob model. A significant caveat to the IMAGE EUV observations is that because of the sensitivity of the cameras, only relatively dense plasmaspheric plasma regions in the outer plasmasphere are observed. It has been estimated that the minimum density observable by IMAGE EUV is $\approx$30 cm^{-3} [*Goldstein et al.*, 2003; *Moldwin et al.*, 2003]. Therefore dense plasmaspheric plasma that exists at L shells above 5 most often would not be observable by IMAGE EUV except during intervals of relatively prolonged quiet when the plasmasphere can reach saturation levels at high L shells [e.g., *Carpenter and Anderson*, 1992; *Sheeley et al.*, 2001].

[3] Early observational studies found an absence of dense plasmaspheric-like regions beyond the plasmapause in the midnight-to-dawn sector [e.g., *Chappell*, 1974]. However, observations at geosynchronous orbit found dense plasmaspheric-like plasma at midnight during intervals of tail stretching in the growth phase of substorms [*Moldwin et al.*, 1996] and during times of quiet geomagnetic activity [e.g., *Moldwin et al.*, 1994].

[1]Institute of Geophysics and Planetary Physics and Department of Earth and Space Sciences, University of California, Los Angeles, California, USA.
[2]Department of Physics, Loyola Marymount University, Los Angeles, California, USA.
[3]Department of Physics and Space Sciences, Florida Institute of Technology, Melbourne, Florida, USA.
[4]Department of Physics and Astronomy, University of Iowa, Iowa City, Iowa, USA.
[5]Department of Information and Systems Engineering, Faculty of Engineering, Graduate School of Natural Science and Technology, Kanazawa University, Kanazawa, Japan.

0148-0227/04/2003JA010320$09.00

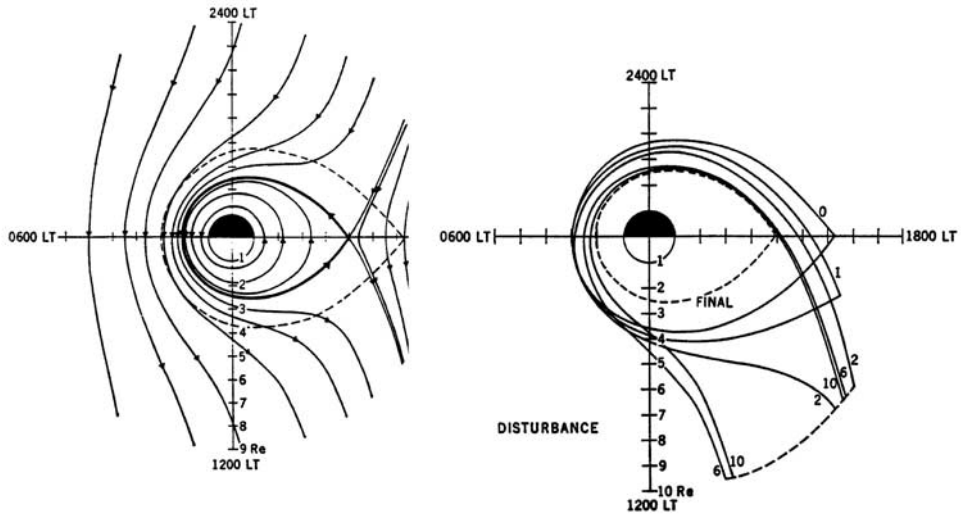

Figure 1. Plume formation modeled with a time-varying convection electric field. From *Grebowsky* [1970].

[4] Therefore some of the outstanding questions in outer plasmaspheric structure that can be addressed by in situ observations are: How often are there plasmaspheric plumes? What is the density structure of plasmaspheric plumes? What is the formation process of plasmaspheric plumes? The answers to these questions are important since recent studies using the IMAGE and Los Alamos National Laboratory geosynchronous spacecraft have indicated that plasmaspheric plumes play a crucial role in midlatitude ionospheric density enhancements [*Foster et al.*, 2002] and polar ionization patches [*Su et al.*, 2001] and are strongly correlated with the loss of ring current ions [*Brandt et al.*, 2002].

[5] The purpose of this study is to determine the properties of plasmaspheric-like plasma beyond the inner plasmapause using the CRRES plasma wave receiver data set. The CRRES spacecraft provides the most extensive database of in situ observations of plasmaspheric density structure and dynamics to date. We use the database of plasmapause locations identified by *Moldwin et al.* [2002] and the empirical plasmaspheric and trough density models developed by *Sheeley et al.* [2001]. Both of these studies used the CRRES plasma wave receiver density database that this study utilizes. These regions will be referred to as plumes for simplicity even though in situ observations cannot determine if the high-density regions beyond the inner plasmasphere are detached (blobs) or connected (plumes).

2. Methodology

2.1. Instrumentation and Description of Data

[6] This study used plasma density data inferred by the plasma wave instrument on the CRRES satellite. This data set spanned 20 August 1990 to 12 October 1991. CRRES had a geosynchronous transfer orbit (an elliptical orbit with a perigee of 1.05 R_E and an apogee of 6.26 R_E with respect to the center of the Earth), with an inclination of 18.15°. Because of the inclination, CRRES was able to sample L shells up to 8 on occasion. The apogee of CRRES precessed from 1000 to 1400 LT through midnight before its failure. Because of the upper frequency limit of the instrument the maximum plasma density that could be measured was $\approx$2000 cm^{-3}. This limited the usable data to L shells generally above 2 [e.g., *Anderson et al.*, 1992; *Sheeley et al.*, 2001]. Because of the early failure of CRRES, not all local times and all L shells were covered. Most importantly, the high-L shell dayside outer plasmasphere was not sampled. In addition, significant data gaps exist in the midnight local time sector.

2.2. Plasmapause Selection

[7] This study used the database of plasmapause locations identified by *Moldwin et al.* [2002]. Briefly, that study identified the innermost steep density gradient in the density profile as the plasmapause. A factor of 5 drop within half an L shell was required. Of the 1328 CRRES inbound and outbound orbit trajectories that had data coverage, 969 (73%) had a plasmapause identified. For this study, the CRRES plasmapause database is examined in terms of complete orbits (i.e., CRRES orbits in which there was data coverage for both the inbound and outbound trajectories). This was done to clearly identify plasmaspheric-like density regions "outside" the main plasmasphere. Organized in this way, of the 1006 total CRRES orbits, 558 had complete data coverage and at least 1 plasmapause per orbit. This database was used to quantitatively identify regions of dense plasmaspheric plasma that were located outside the main plasmapause.

2.3. Plume Interval Selection

[8] The selection of the regions of plasmaspheric-like plasma beyond the plasmapause was made using the empirical models of *Sheeley et al.* [2001]. These models, which are based on the CRRES data set, describe the plasmasphere and the trough number densities in the region $3 \leq L \leq 7$ as a function of L shell and magnetic local time.

[9] In the plasmasphere model the average number density (in cm^{-3}) as a function of L shell is given by

$$n_p = 1390(3/L)^{4.83} \pm 440(3/L)^{3.60}, \quad (1)$$

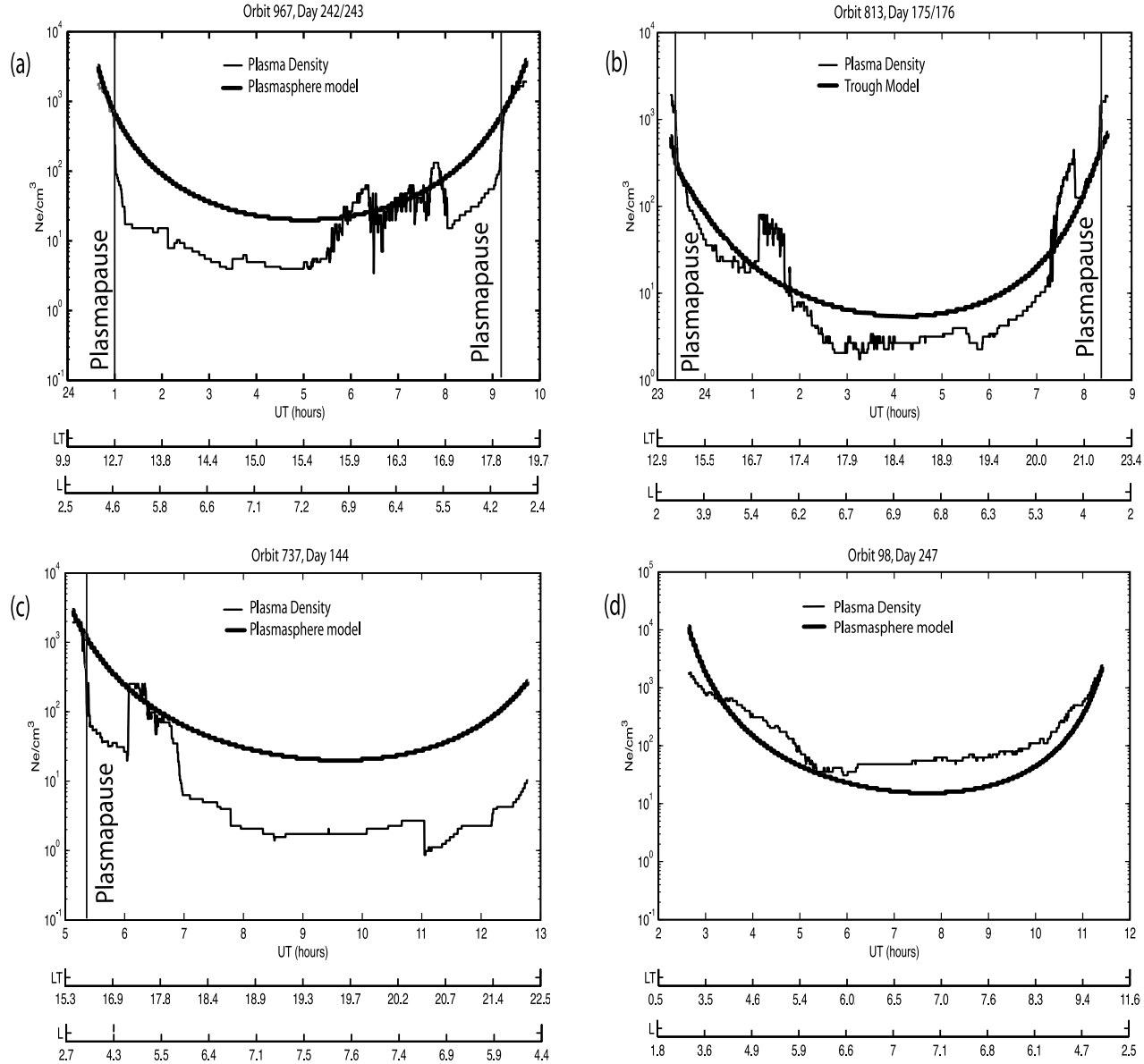

Figure 2. Examples of the plume selection methodology. The thick curve shows the scaled *Sheeley et al.* [2001] trough or plasmasphere model used to identify intervals. The vertical lines show the location of the plasmapause as determined by *Moldwin et al.* [2002]. Figure 2d shows an example where there was no clear plasmapause identified. These cases were not included in this survey.

where 1390 cm^{-3} is the average number density of the plasmasphere at $L = 3$, which falls off at a rate of $L^{-4.83}$. The standard deviation at $L = 3$ is ≈440 cm^{-3}, and this falls off at a rate of $L^{-3.60}$.

[10] In the trough model the average number density is given by

$$n_t = 124(3/L)^{4.0} + 36(3/L)^{3.5}\cos\left(\left\{\mathrm{LT} - \left[7.7(3/L)^{2.0} + 12\right]\right\}/12\right) \pm \left\{78(3/L)^{4.72} + 17(3/L)^{3.75}\cos[(\mathrm{LT} - 22)/12]\right\}, \quad (2)$$

where 124 cm^{-3} is the average number density of the trough at $L = 3$, which falls off at a rate of $L^{-4.0}$. The CRRES data indicate that there is a sinusoidal variation of the trough density as a function of local time, and this is also included in equation (2).

[11] In this study, we use L of 3 as a dividing line for whether to use the plasmasphere or trough model in selecting the plasmaspheric intervals located outside the plasmapause. If the plasmapause is located earthward of L of 3, we define plasmaspheric plume intervals to be those whose density exceeds the trough plus 1σ density of the *Sheeley et al.* [2001] model. If the plasmapause is located outside of L of 3, we define plasmaspheric plumes to be those whose density exceeds the Sheeley et al. plasmaspheric model. These models are scaled to each orbit to account for the wide variability in the plasmaspheric density from day to day. The average density of the two points of each orbit at $L = 3$ is used as the scaling factor for equations (1) and (2) (i.e., instead of using 1390 or 124 cm^{-3} as the leading term, the average density at $L = 3$ observed during the actual orbit is used). If the orbit had only one clearly identified

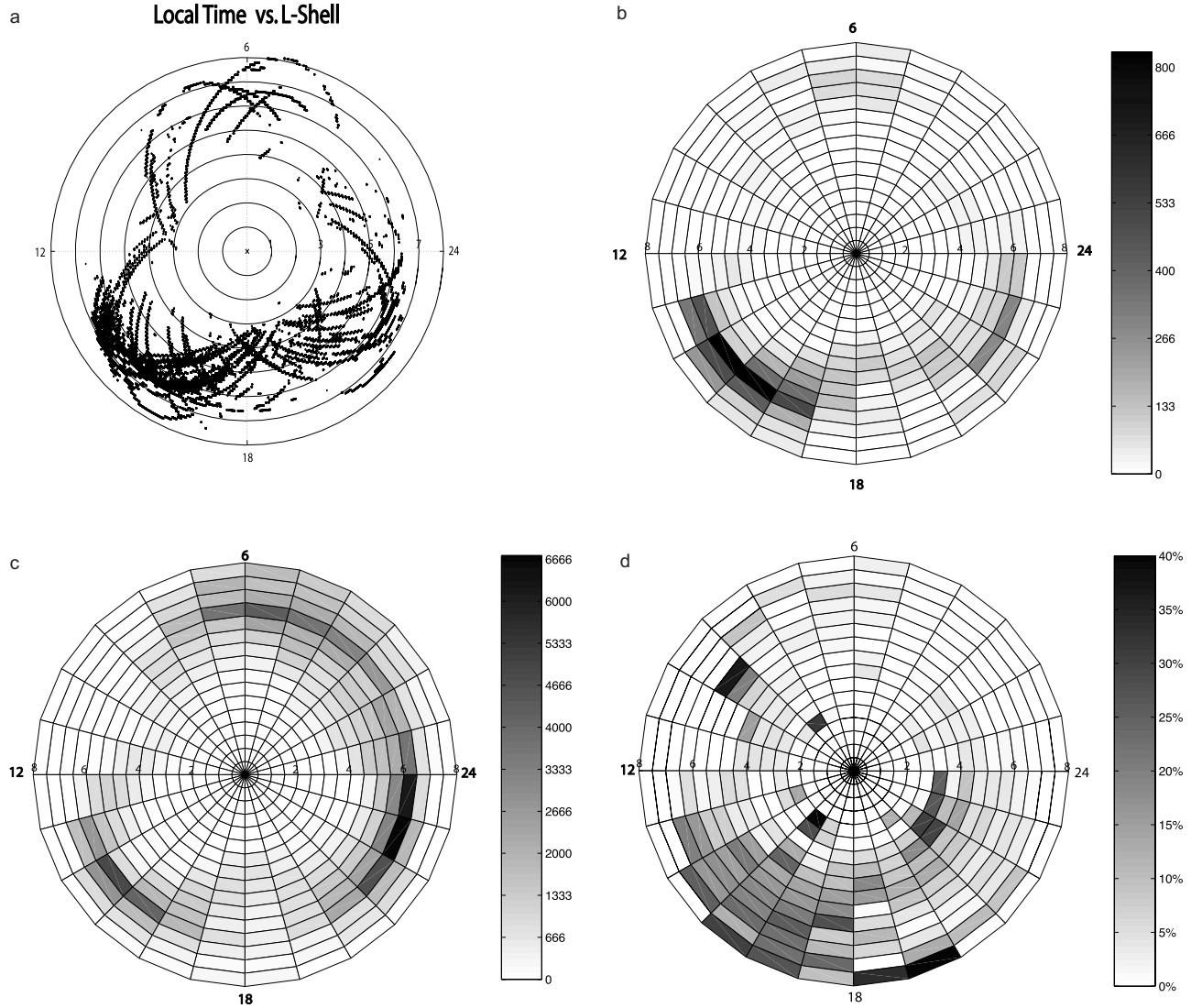

Figure 3. (a) Location of density data points within a plume interval as a function of local time and L shell. (b) Total duration of plume intervals (in minutes) in 0.5 L shell by 1 hour of LT bins. (c) Total amount of time CRRES observed trough densities in the same format as Figure 3b. Most trough intervals were observed on the nightside. (d) Normalized occurrence frequency of the plume intervals normalized to the total time of trough observations in 0.5 L shell by 1 hour of LT bins. Note the relatively high occurrence frequency of plumes in the noon-to-dusk sector.

plasmapause (observed during either the outbound or the inbound portion of the orbit), the scaling factor was the density at L of 3 on the portion of the orbit where the plasmapause was observed.

[12] The criterion used to select a plume was that the interval's density had to exceed the model value of the plasmasphere (or trough plus 1σ) density over a minimum of eight consecutive observations (a duration of $\approx$1 min). Furthermore, two adjacent plumes were considered to be separate intervals if they were separated by at least eight observations in which the trough density fell below the model plasmasphere density. Figure 2a shows an example of an orbit with two plasmapause observations, both beyond $L = 3$. The model plasmasphere density is indicated by the thick curve, and the vertical lines show the locations of the plasmapauses. Figure 2b is an example of an orbit with the plasmapauses located earthward of L of 3, while Figure 2c is an example of an orbit with only one plasmapause clearly identified.

[13] The absence of a plasmapause may indicate that either CRRES remained within the plasmasphere throughout the entire orbit or no clear sharp density gradient was observed. These orbits were excluded from our study. An example of such an orbit is shown in Figure 2d.

3. Results

3.1. Occurrence of Plumes

[14] This study found that 169 of the 558 (30%) complete orbits with at least one identifiable plasmapause exhibited plasmaspheric-like plasma density structures beyond the plasmapause. There were 788 plume intervals during the

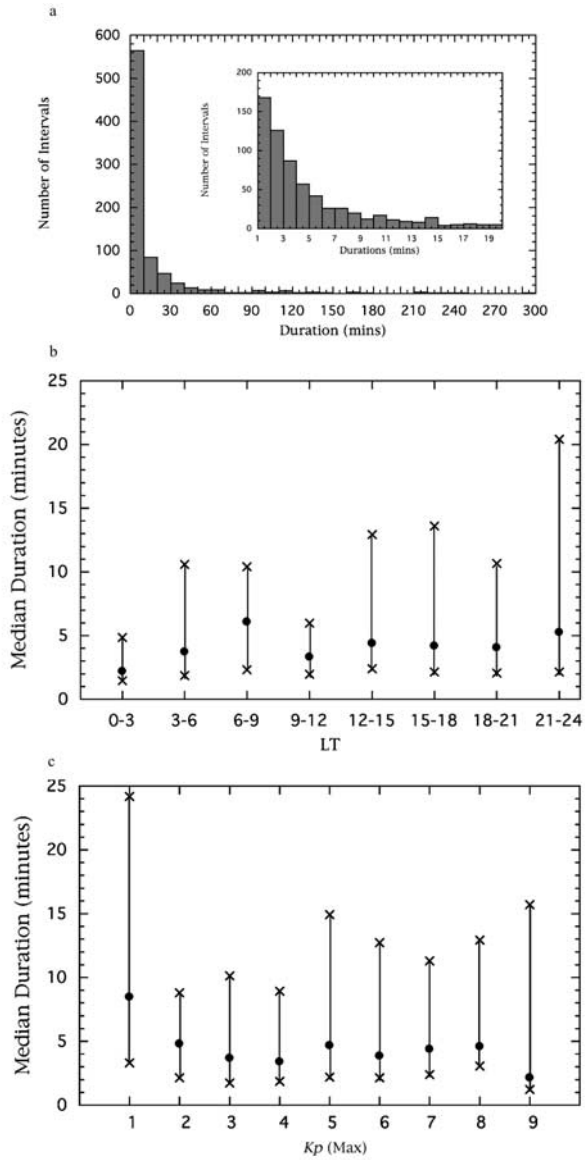

Figure 4. (a) Distribution of the duration of plasmaspheric plume intervals as observed by CRRES. Note that most intervals are <10 min in duration. (b) Median duration (in minutes) of the plasmaspheric plumes as a function of local time. Error bars show the upper and lower quartiles. (c) Median duration (in minutes) of the plasmaspheric plumes as a function of the maximum *Kp* in the previous 12 hours. Error bars show the upper and lower quartiles.

169 orbits with high-density structures. On 55 (or 33%) of the orbits with plumes, plumes appeared in consecutive orbits, whereas the remaining orbits that contained plumes did not have a plume observation during the previous or next orbit.

3.2. Location of Plumes in *L* Shell and LT

[15] Each density record beyond the innermost plasmapause from the CRRES mission was compared with the appropriately scaled *Sheeley et al.* [2001] trough or plasmasphere model as described in section 2.3. Figure 3a shows the local time and *L* shell location of the dense plasmaspheric plasma intervals selected in this study. Figure 3b shows the total time that CRRES observed plume intervals in 0.5 *L* shell by 1 hour of LT bins in minutes. Figure 3c shows the total amount of time CRRES observed trough intervals in the same format as Figure 3b. Figure 3d shows the normalized (by the amount of time of trough observations in that bin, i.e., total time outside the main plasmapause) occurrence frequency of dense plasmaspheric plasma beyond the main plasmapause in 0.5 *L* shell by 1 hour of LT bins. Note that plasmaspheric plumes can occur at essentially all local times, though they occur most often in the noon-to-dusk sector.

3.3. Average and Median Duration of Plumes

[16] The distribution of the duration of the plume intervals is shown in Figure 4a. The duration of a plume interval is determined by the length of time the density exceeded the model plasmasphere threshold during a single orbit. The average duration is 15.24 ± 32.46 min, with a maximum duration of 4 hours and 53 min. However, as can be seen in Figure 4a, most intervals had durations of <10 min. The Figure 4a inset shows the same data as in the larger histogram but binned at a finer resolution. This shows that the median value of duration is 4.1 min. The median duration of the plumes as a function of local time is examined in Figure 4b. Most intervals had an average duration of ≈4 min, and there is no significant variation of the mean as a function of local time. Figure 4c examines the median duration as a function of geomagnetic activity as indicated by maximum *Kp* in the previous 12 hours. Note that there is a statistically significant dependence on geomagnetic activity for the duration of each plume event, with the longer durations for the lowest levels of geomagnetic activity.

3.4. Average Density

[17] Figure 5a shows the density of each point identified as part of a plume as a function of *L* shell. Overlaid on these data are the model curves from the unscaled *Sheeley et al.* [2001] plasmasphere model. Figure 5b examines the difference in density of each selected plume interval compared with the model "plasmaspheric-like" density (either the Sheeley et al. trough plus 1σ or the plasmasphere model, depending on the location of the plasmapause) as a function of local time. These delta densities show that most plume intervals are significantly higher than the selection criterion, particularly in the nightside trough region. An inspection of the individual events found that most of the density gradients between the plumes and the background trough are plasmapause-like (see, e.g., Figures 2a, 2b, and 2c).

3.5. Occurrence Frequency as a Function of Geomagnetic Activity

[18] Figure 6a shows the distribution of geomagnetic activity as indicated by maximum *Kp* in the previous 12 hours for the plume intervals. Also plotted is the distribution of *Kp* maximum in any given 12-hour interval during the entire CRRES interval (note the different scale for the two distributions). The two distributions are offset, with the plume intervals appearing during times of enhanced geomagnetic activity. To emphasize this trend, Figure 6b examines the normalized occurrence frequency

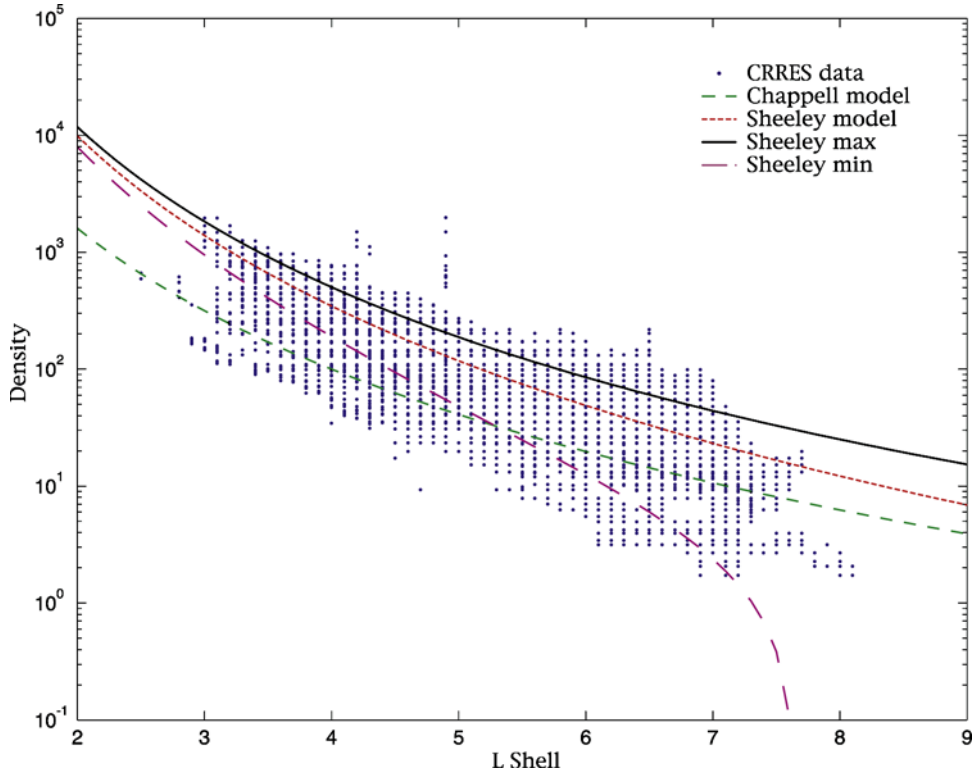

Figure 5a. Density of the plume intervals as a function of L shell. The unscaled *Sheeley et al.* [2001] plasmasphere and $\pm 1\sigma$ curves and the *Chappell* [1974] density criteria are also shown. Note that the actual selection criteria used scaled values of these curves as well as the trough model that had a local time dependency (not shown).

of the plumes as a function of the overall maximum *Kp*. Note that plume intervals are observed over 50% of the time when *Kp* is high. Figure 7 shows the minimum *Dst* in the previous 24 hours for the plume intervals. A majority of the plume intervals occur when *Dst* does not go below −50 nT, though the most probable minimum *Dst* is between −25 and −50 nT, indicating possible dependence on weak geomagnetic storms.

[19] Plumes occur during periods of moderate to disturbed intervals but often persist well into the recovery phase. A storm (as indicated by $Dst < -50$ nT) is not needed to create a plume, but enhanced convection (as indicated by $Kp \geq 3$) does seem to be sufficient to generate plumes.

[20] Figure 8 shows three consecutive inbound orbits of CRRES following a storm on 9 September 1991. A storm sudden commencement (SSC) occurred between the plasmapause crossings observed on orbits 990 and 991. Note prior to the SSC (orbit 990) the absence of plasmaspheric plumes, while during orbits 991 and 992, dense plasmaspheric plumes appear at high L beyond the plasmapause. These three orbits are separated in time by ≈10 hours (the CRRES orbital period). The SSC occurs at the very end of orbit 990 and ≈7 hours before the beginning of the outbound leg of orbit 991. Therefore the structure appeared in this example within 7 hours after the SSC and persisted through orbit 993 (not shown), nearly 24 hours after the first appearance of the plume. The local time location of apogee from orbit to orbit changes by <15 min; therefore the orbit-to-orbit changes observed are due to plasmapause and plume structure evolution, not motion through a different local time sector. It should be noted that this example shows that the innermost plasmapause moves outward in response to the storm. This is opposite to the classic plasmapause motion picture. However, this example is in the dusk sector following a storm, and *Moldwin et al.* [2003] found that plasmapause motion in response to storms is highly local time-dependent. The dusk sector shows highly variable plasmapause motion, including both radial inward and outward motion. Only in the nightside and dawn sectors

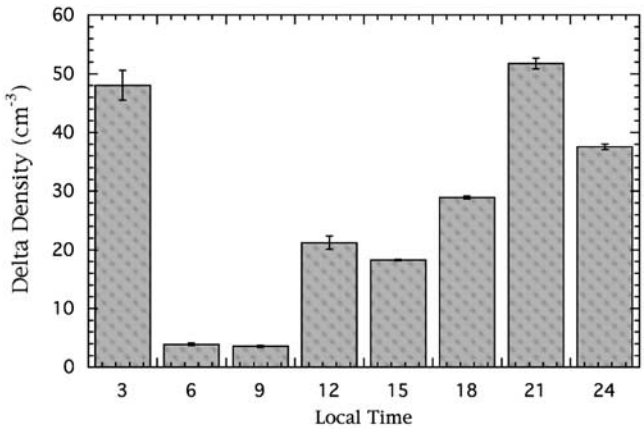

Figure 5b. Difference in density of the plasmaspheric plume compared with the appropriate *Sheeley et al.* [2001] plasmasphere or trough model as a function of local time. Error bars are the normalized standard deviation ($\sigma/\sqrt{n}$).

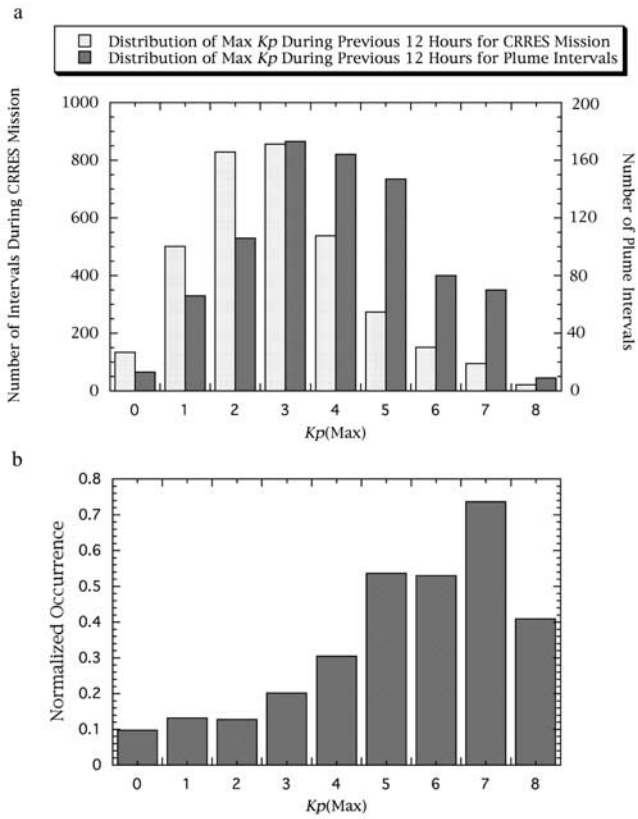

Figure 6. (a) Comparison of the occurrence distributions of plumes versus the distribution of geomagnetic activity as indicated by maximum *Kp* in the previous 12 hours for the entire CRRES mission. Note the different scale for the two different distributions. (b) Normalized occurrence of plume intervals as a function of maximum *Kp* during the previous 12 hours.

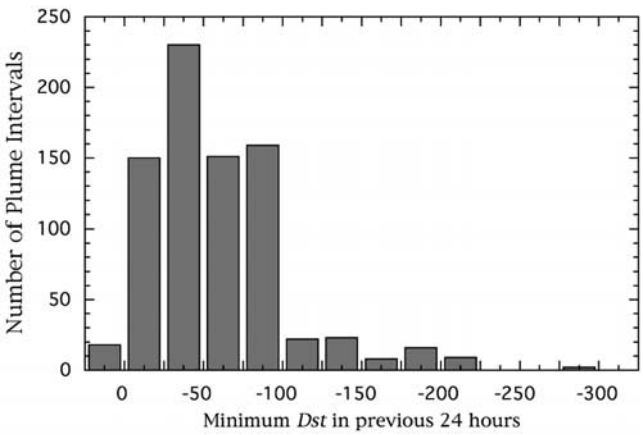

Figure 7. Distribution of the number of events as a function of minimum *Dst* in the previous 24 hours. Each bin contains intervals that had a minimum *Dst* greater than the value given on the axis (i.e., the first bin on the left contains all plume intervals that had a minimum *Dst* of 0 nT or greater).

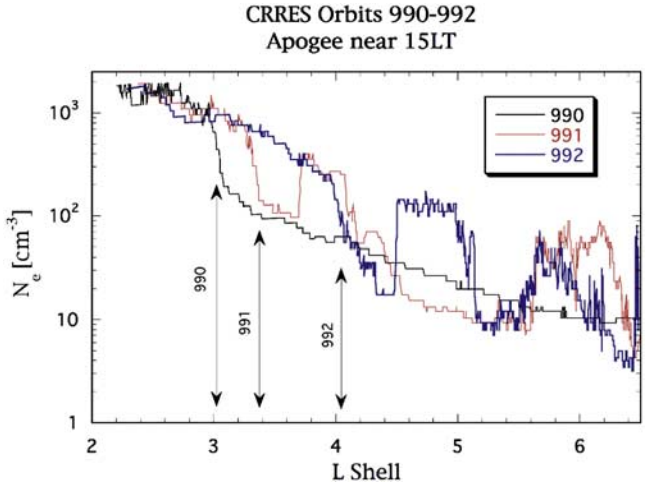

Figure 8. Example of the appearance of plasmaspheric plumes following a storm [from *Moldwin et al.*, 2003]. The vertical lines with orbit numbers indicate plasmapause locations.

(2100 to 0900 LT) is the classic inward motion in response to storms exclusively observed.

4. Discussion

[21] The outer magnetosphere often contains dense plasmaspheric plasma that extends beyond the main plasmasphere. This plasma most often appears in the noon-to-dusk sector in the aftermath of enhanced geomagnetic activity, but density structure is observed at other local times as well. This finding is in contrast to the study of *Chappell* [1974] that examined OGO 5 data and found an absence of dense plasmaspheric plasma beyond the plasmapause in the midnight-to-dawn sector.

[22] An examination of our data set using the *Chappell* [1974] selection criteria of having the density exceed a level of 100 cm^{-3} at an L of 4 falling off as L^{-4} found that 86% of our data points meet this criterioa. (The Chappell density criterion model curve is shown in Figure 5a.) The 14% of the points in our study that did not exceed the *Chappell* [1974] criteria were distributed in local time similarly to the overall population. The OGO 5 measurements were made using a light ion mass spectrometer, and the H^+ density was examined by *Chappell* [1974]. The CRRES data set is from the plasma wave receiver's measurement of either the electron plasma frequency (f_{pe}) or the upper hybrid resonance frequency ($f_{UHR} = \sqrt{f_{pe} + f_{ce}}$, where f_{ce} is the electron cyclotron frequency), which yields the total electron number density independent of spacecraft potential. We suggest that the difference in our results is due to incomplete counting of the total electron density of OGO 5's mass spectrometer results due to spacecraft potential effects in the low-density nightside trough and/or the presence of heavy ions.

[23] Observations from IMAGE EUV and the Radio Plasma Imager show that plumes have extensive longitudinal extent [*Garcia et al.*, 2003]. As Figure 8 shows, plumes can be long-lived, with dense plasma being observed over several 10-hour orbits (with the assumption that the plume intervals observed from orbit to orbit are the same plume

structures). We find that plumes can appear quickly in the aftermath of enhanced activity and persist for over a day. The rapidity of the formation of the plume is consistent with the ≈1-hour response time of the motion of the location of the plasmapause following an SSC. This was found in a superposed epoch study of CRRES plasmapause dynamics [*Moldwin et al.*, 2003].

5. Conclusions

[24] We found that plasmaspheric plumes are a common feature of the inner magnetosphere and tend to appear in the aftermath of enhanced geomagnetic activity. The density of the plumes is such that they have plasmaspheric-like density gradients between the surrounding trough.

[25] Though in situ observations cannot uniquely discriminate between plumes and detached blobs, most of the observations are consistent with the plume formation model. This model predicts that most observations should be in the noon-to-dusk sector in the aftermath of enhanced geomagnetic activity. Observations in the midnight and dawn sides are not clearly explained by this model, though some modeling studies [*Ober et al.*, 1997] suggest that plumes can corotate to the nightside. In addition, recent IMAGE EUV observations [*Spasojevic et al.*, 2003] have shown tails or plumes wrapping around midnight during the recovery phase of a storm. Since ring current loss through direct Coloumb interaction and the enhancement of wave scattering is important for understanding storm development and ring current modeling, this study suggests that models need to incorporate the presence of plasmaspheric plumes in order to properly understand the inner magnetosphere.

[26] **Acknowledgments.** The work at UCLA and Florida Tech was partially supported by a NASA SR&T grant (NAGW-5153 and NAG5-4897), while NSF grant ATM-0089718 supported the contributions made at LMU. The authors thank David Berube for his help in MATLab programming and data visualization.

[27] Arthur Richmond thanks Leonard Garcia and Yi-Jiun Su for their assistance in evaluating this paper.

References

Anderson, R. R., D. A. Gurnett, and D. L. Odem (1992), The CRRES plasma wave experiment, *J. Spacecr. Rockets*, *29*, 570.

Brandt, P. C., D. G. Mitchell, Y. Ebihara, B. R. Sandel, E. C. Roelof, J. L. Burch, and R. Demajistre (2002), Global IMAGE/HENA observations of the ring current: Examples of rapid response to IMF and ring-current plasmasphere interaction, *J. Geophys. Res.*, *107*(A11), 1359, doi:10.1029/2001JA000084.

Carpenter, D. L., and R. R. Anderson (1992), An ISEE/whistler model of equatorial electron density in the magnetosphere, *J. Geophys. Res.*, *97*, 1097.

Carpenter, D. L., B. L. Giles, C. R. Chappell, P. M. E. Décréau, R. R. Anderson, A. M. Persoon, A. J. Smith, Y. Corcuff, and P. Canu (1993), Plasmasphere dynamics in the duskside bulge region: A new look at an old topic, *J. Geophys. Res.*, *98*, 19,243.

Chappell, C. R. (1974), Detached plasma regions in the magnetosphere, *J. Geophys. Res.*, *79*, 1861.

Chen, A. J., and J. M. Grebowsky (1978), Dynamical interpretation of observed plasmasphere deformations, *Planet. Space Sci.*, *26*, 661.

Chen, A. J., and R. A. Wolf (1972), Effects on the plasmasphere of a time-varying convection electric field, *Planet. Space Sci.*, *20*, 483.

Elphic, R. C., L. A. Weiss, M. F. Thomsen, D. J. McComas, and M. B. Moldwin (1996), Evolution of plasmaspheric ions at geosynchronous orbit during times of high geomagnetic activity, *Geophys. Res. Lett.*, *23*, 2189.

Foster, J. C., P. J. Erickson, A. J. Coster, J. Goldstein, and F. J. Rich (2002), Ionospheric signatures of plasmaspheric tails, *Geophys. Res. Lett.*, *29*(13), 1623, doi:10.1029/2002GL015067.

Garcia, L. N., S. F. Fung, J. L. Green, S. A. Boardsen, B. R. Sandel, and B. W. Reinisch (2003), Observations of the latitudinal structure of plasmaspheric convection plumes by IMAGE-RPI and EUV, *J. Geophys. Res.*, *108*(A8), 1321, doi:10.1029/2002JA009496.

Goldstein, J., B. R. Sandel, W. T. Forrester, and P. H. Reiff (2003), IMF-driven plasmasphere erosion of 10 July 2000, *Geophys. Res. Lett.*, *30*(3), 1146, doi:10.1029/2002GL016478.

Grebowsky, J. M. (1970), Model study of plasmapause motion, *J. Geophys. Res.*, *75*, 4329.

Green, J. L., B. R. Sandel, S. F. Fung, D. L. Gallagher, and B. W. Reinisch (2002), On the origin of kilometric continuum, *J. Geophys. Res.*, *107*(A7), 1105, doi:10.1029/2001JA000193.

Higel, B., and W. Lei (1984), Electron density and plasmapause characteristics at 6.6 RE: A statistical study of the GEOS 2 relaxation sounder data, *J. Geophys. Res.*, *89*, 1583.

Lemaire, J. F. (2000), The formation plasmaspheric plumes, *Phys. Chem. Earth, Part C*, *25*, 9.

Moldwin, M. B., M. F. Thomsen, S. J. Bame, D. J. McComas, and K. R. Moore (1994), An examination of the structure and dynamics of the outer plasmasphere using multiple geosynchronous satellites, *J. Geophys. Res.*, *99*, 1475.

Moldwin, M. B., M. F. Thomsen, S. J. Bame, D. J. McComas, L. A. Weiss, G. D. Reeves, and R. Belian (1996), The appearance of plasmaspheric plasma in the outer magnetosphere in association with the substorm growth phase, *Geophys. Res. Lett.*, *23*, 801.

Moldwin, M. B., L. Downward, H. K. Rassoul, R. Amin, and R. R. Anderson (2002), A new model of the location of the plasmapause: CRRES results, *J. Geophys. Res.*, *107*(A11), 1339, doi:10.1029/2001JA009211.

Moldwin, M. B., S. Mayerberger, H. K. Rassoul, T. Barnicki, and R. R. Anderson (2003), Plasmapause response to geomagnetic storms: CRRES results, *J. Geophys. Res.*, *108*(A11), 1399, doi:10.1029/2003JA010187.

Ober, D. M., J. L. Horwitz, M. F. Thomsen, R. C. Elphic, D. J. McComas, R. D. Belian, and M. B. Moldwin (1997), Premidnight plasmaspheric "plumes,"*J. Geophys. Res.*, *102*, 1325.

O'Brien, T. P., and M. B. Moldwin (2003), Empirical plasmapause models from magnetic indices, *Geophys. Res. Lett.*, *30*(4), 1152, doi:10.1029/2002GL016007.

Sandel, B. R., R. A. King, W. T. Forrester, D. L. Gallagher, A. L. Broadfoot, and C. C. Curtis (2001), Initial results from the IMAGE Extreme Ultraviolet Imager, *Geophys. Res. Lett.*, *28*, 1439.

Sheeley, B. W., M. B. Moldwin, H. K. Rassoul, and R. R. Anderson (2001), An empirical plasmasphere and trough density model: CRRES observations, *J. Geophys. Res.*, *106*, 25,631.

Spasojevic, M., J. Goldstein, D. L. Carpenter, U. S. Inan, B. R. Sandel, M. B. Moldwin, and B. W. Reinisch (2003), Global response of the plasmasphere to a geomagnetic disturbance, *J. Geophys. Res.*, *108*(A9), 1340, doi:10.1029/2003JA009987.

Su, Y.-J., M. F. Thomsen, J. E. Borovsky, and J. C. Foster (2001), A linkage between polar patches and plasmaspheric drainage plumes, *Geophys. Res. Lett.*, *28*, 111.

Taylor, H. A., H. C. Brinton, and A. R. Deshmukh (1970), Observations of irregular structure in thermal ion distributions in the duskside magnetosphere, *J. Geophys. Res.*, *75*, 2481.

R. R. Anderson, Department of Physics and Astronomy, University of Iowa, 203 Van Allen Hall, Iowa City, IA 52242-1479, USA. (anderson@iowave.physics.uiowa.edu)

J. D. Bocchicchio and H. K. Rassoul, Department of Physics and Space Sciences, Florida Institute of Technology, 150 West University Blvd., Melbourne, FL 32901, USA. (jennybo@bigfoot.com; rassoul@pss.fit.edu)

J. Howard and J. Sanny, Department of Physics, Loyola Marymount University, Seaver Hall, One LMU Drive, MS 8227, Los Angeles, CA 90045-2659, USA. (iamjohnahoward@hotmail.com; jsanny@lmu.edu)

M. B. Moldwin, IGPP, University of California, 3845 Slichter Hall, Los Angeles, CA 90095-1567, USA. (mmoldwin@igpp.ucla.edu)